FIRST VERTICAL TEST OF SUPERCONDUCTING QWR PROTOTYPE AT RIKEN

K. Yamada*, O. Kamigaito, K. Ozeki, N. Sakamoto, K. Suda, Y. Watanabe,
RIKEN Nishina Center, Wako, Saitama, Japan
E. Kako, H. Nakai, K. Umemori, KEK, Tsukuba, Ibaraki, Japan
A. Miyamoto, K. Sennyu, T. Yanagisawa,
Mitsubishi Heavy Industries Mechatronics Systems, Ltd. (MHS-MS), Kobe, Hyogo, Japan

Abstract

The assembly of a prototype of the RIKEN superconducting quarter-wavelength resonator was completed in June 2016, and the first vertical test of the prototype has been performed at KEK. As a result, acceptably high values of Q_0 and E_{acc} have been achieved. This paper presents the results of the first vertical test as well as the preparation and test procedures.

INTRODUCTION

A CW high-intensity ion accelerator is one of the candidates for a system aimed at reducing the amount of long-lived fission products (LLFP) in high-level radioactive waste by converting LLFP nuclides into short-lived or stable nuclides through nuclear transmutation. For such a transmutation system, efficient acceleration of the ion beam with an intensity greater than 100 mA is required. A superconducting linear accelerator is one of the most promising candidates for realizing such high-intensity ion acceleration. As described in Ref. [1], fabrication of the first prototype of a superconducting quarter-wavelength resonator (SC-QWR) was started at RIKEN Nishina Center last year, in order to develop elemental technologies required for the low-velocity part of the CW high-intensity ion linear accelerator.

FABRICATION OF SC-QWR PROTOTYPE

Figure 1 shows cross-sectional views of the SC-QWR prototype. The design parameters of the prototype SC-QWR are summarized in Table 1. The SC-QWR prototype was made from a bulk Nb sheet with a residual resistance ratio (RRR) of 250. A half-cell comprising the drift tube and stem was formed by stamping them into one piece, as described in Ref. [2]. After the production of its partial components, i.e. the outer cylinder, stem, upper torus, and bottom dome, the resonant frequency of their assembly was measured and careful adjustments were made to the straight section of the top part of the outer cylinder as well as the stem and bottom side of the outer cylinder. The final assembly of the SC-QWR prototype by electron beam welding was completed in June 2016. Photographs of the part and the completed SC-QWR prototype are shown in Fig. 2.

The first cool-down test of the SC-QWR prototype along with the startup of a newly constructed vertical test stand

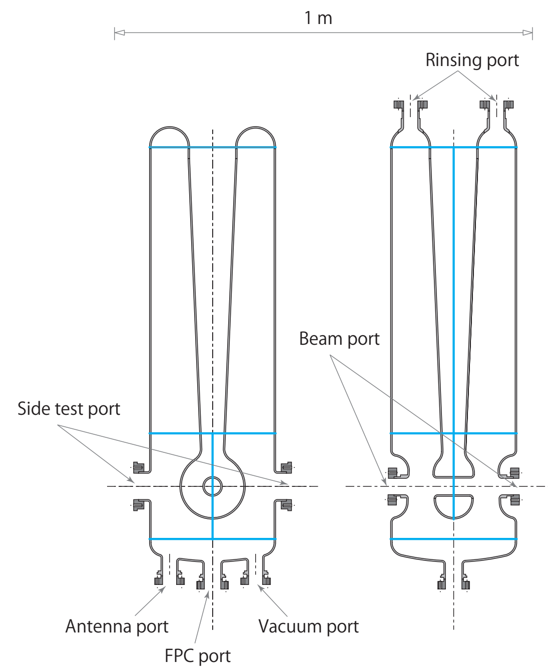

Figure 1: Designed schematics of the SC-QWR prototype.

Table 1: Design Parameters of the SC-QWR Prototype. Surface Resistance was Assumed to be 25 nΩ in the Calculation

Frequency [MHz] at 4.5 K	75.5
Duty [%]	100
β_{opt}	0.08
G [Ω]	23.5
R_{sh}/Q_0 [Ω]	578
Q_0	9.4×10^8
P_0 [W]	3.8
V_{acc} [MV] at E_{acc} = 4.5 MV/m, β = 0.08	1.44
E_{acc} [MV/m]	4.5
E_{peak}/E_{acc}	6.2
B_{peak}/E_{acc} [mT/(MV/m)]	9.7

was performed after a test of the buffered chemical polishing (BCP) and high-pressure rinsing (HPR) system [3]. Subsequently, surface treatments of BCP1 (100 μm), annealing, BCP2 (20 μm), ultrasonic cleaning, HPR, and baking were performed sequentially from July through August in 2016. After overcoming several problems with the vertical test stand, the first vertical test was successfully carried out in September 2016.

* nari-yamada@riken.jp

ISBN 978-3-95450-169-4

Figure 2: Photographs of the stem (upper left), inner view (middle left), top torus (lower left), bottom dome (lower right), and outward (upper right) of the SC-QWR prototype.

VERTICAL TEST STAND

We prepared a vertical test stand for the SC-QWR prototype at KEK. A pit, cryostat chamber, and magnetic shield were reused for the test stand with some modifications. The inner dimensions of the cryostat are ϕ600 mm diameter and 2420 mm depth. The upper torus of the SC-QWR prototype is located approximately 1050 mm below the top flange. The top flange and hanger apparatus for the test assembly were newly produced to fit the SC-QWR prototype. Initially, the Mu-metal magnetic shield surrounded the exterior of the cryostat and the residual magnetic field in the vicinity of the upper torus was measured to be 60 mG. After the installation of an additional extension of the Mu-metal shield, the residual magnetic field was reduced to 30 mG. It should be noted that the residual magnetic field at the lower part of the cryostat was less than 10 mG for both cases. We also built a clean booth to hang and connect the SC-QWR prototype to the test assembly.

Figure 3 shows the test assembly being installed into the cryostat. For the test assembly, twelve Si-diode thermal sensors were attached to the SC-QWR prototype. Liquid He level sensors were installed both in the cryostat and inside the stem of the SC-QWR prototype. An input coupler for the vertical test was designed with a stroke of $\pm$10 mm, which can change the external quality factor ($Q_{\rm in}$) by the order of 10^2. The rf and radiation interlock, data acquisition excepting the thermometer and rf circuit, and driving of the coupler were implemented on a programmable logic controller.

The rf circuit for the vertical test measurement is shown in Fig. 4. The output power level of the driver amplifier ($P_{\rm in}$), reflection power level from the SC-QWR prototype through a three-port circulator ($P_{\rm ref}$), and transmission power level through the SC-QWR prototype ($P_{\rm t}$) were determined using power meters and their calibration factors. The signal generator rf frequency was tuned to the resonant frequency of the SC-QWR prototype by frequency modulation of a phase lock loop between $P_{\rm in}$ and $P_{\rm t}$. The unloaded quality factor Q_0 of the SC-QWR prototype was deduced by

Figure 3: Test assembly and cryostat.

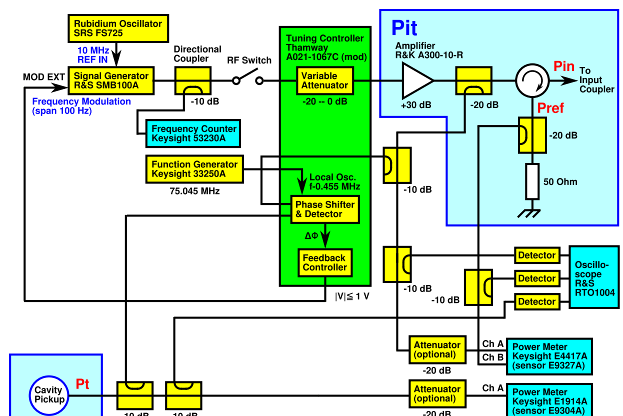

Figure 4: Diagram of the rf circuit for vertical test.

$$
\begin{aligned}
P_0 &= P_{\rm in} - P_{\rm ref} - P_{\rm t}, \\
\beta_{\rm L} &= \frac{1 \pm \sqrt{P_{\rm ref}/P_{\rm in}}}{1 \mp \sqrt{P_{\rm ref}/P_{\rm in}}} \ \text{(over/undercoupling)}, \\
\beta_{\rm t} &= P_{\rm t}/P_0, \\
\beta_{\rm in} &= \beta_{\rm L}(1+\beta_{\rm t}), \\
Q_{\rm L} &= 2\pi f_0 \tau_{1/2}/\ln 2, \\
Q_0 &= Q_{\rm L}(1+\beta_{\rm in}+\beta_{\rm t}),
\end{aligned}
$$

where $\tau_{1/2}$ was obtained from a decay curve of $\mathrm{P_t}$, measured by an oscilloscope. The acceleration field $E_{\rm acc}$ was evaluated by

$$
E_{\rm acc} = \frac{\sqrt{(R_{\rm sh}/Q_0)P_0 Q_0}}{\beta_{\rm opt}\lambda} \ \text{[MV/m]},
$$

where $\beta_{\mathrm{opt}}\lambda = 0.32$ m for the SC-QWR prototype.

RESULTS OF PERFORMANCE TEST

At first, we checked whether the coupling of the input coupler was over or under by observing the envelope of the P_{ref} signal via the oscilloscope. The detected signal at the inner-limit position of the coupler is shown in Fig. 5. The envelope indicated over coupling, as expected by a simulation using CST Microwave Studio (MWS) [4]. The position of the coupler was then swept from the inner limit to the outer limit and Q_{in} was measured, as shown in Fig. 6. The red dots indicate the resultant Q_{in}, where Q_{in} was evaluated by $Q_{\mathrm{in}} = Q_0/\beta_{\mathrm{in}}$.

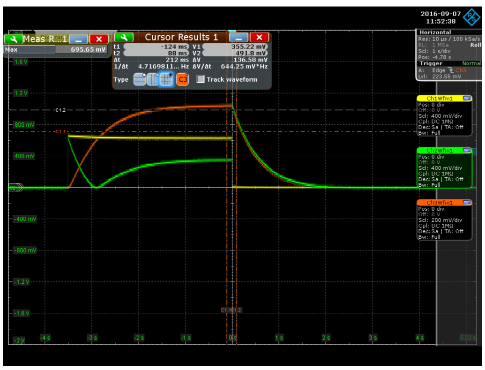

Figure 5: Forward, reflection, and transmission signal when the coupler position was at the inner limit (+10 mm). Green line indicates the reflection signal.

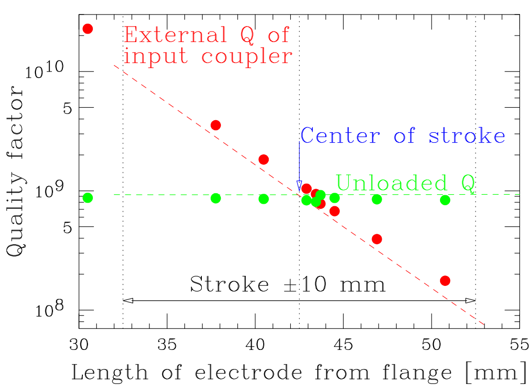

Figure 6: Q_{in} and Q_0 as a function of coupler position. Dashed lines indicate Q_{in} and Q_0 obtained from simulation.

After adjusting the coupler position where coupling was slightly over, we measured the Q_0 value for each E_{acc} level. Figure 7 shows the Q_0 plotted against E_{acc} for three independent runs. An R_{sh}/Q_0 value of 587 Ω was used for the evaluation of E_{acc}, which reflects the actual geometry of the SC-QWR prototype after fabrication. In the first run, the multipactor was observed at 0.9 MV/m, as indicated in the figure. However, it was overcome by rapid ramping of rf power. Although the E_{acc} favorably increased, X-ray emission suddenly occurred at 9.2 MV/m. It should be noted that the P_{in} of 25 W at 9.2 MV/m was considerably higher than the rated power of the driver amplifier. To check the degradation of the SC-QWR prototype due to X-ray emission, a second run was performed and no damage was observed. A third run was performed to process the multipacting with a level at approximately 0.9 MV/m. The multipacting was easily processed within 30 min, as shown in the results of the third run (Fig. 7).

The observed Q_0 values are consistent with the design parameters of the SC-QWR prototype. If we assume a refrigeration capacity of 8 W, the Q_0 value of the SC-QWR prototype is high enough for operation. The maximum E_{acc} is significantly higher than the required value and exponential deterioration of Q_0 has not yet been observed. B_{peak} has a sufficient margin, and therefore higher E_{acc} may potentially be excited.

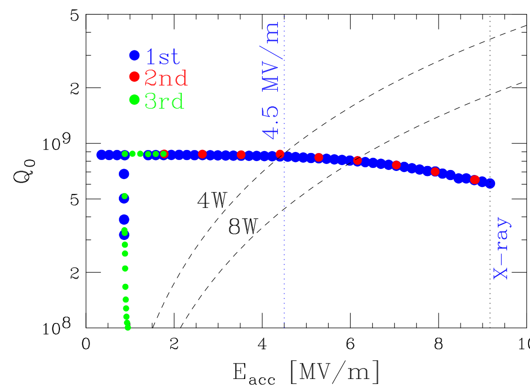

Figure 7: Q_0 vs E_{acc} plot of the SC-QWR prototype for three independent runs.

SUMMARY AND OUTLOOK

The first vertical test of the SC-QWR has been carried out and acceptably high values of Q_0 and E_{acc} have been achieved. We plan to perform the vertical test once more after additional light BCP and HPR treatments. The titanium jacket will be welded onto the SC-QWR prototype. One problem is that the resonant frequency of the SC-QWR prototype, 75.5199 MHz, is slightly out of the range of the tuner. Thus, we plan to correct the frequency by pre-tuning of pressing the SC-QWR prototype to beam port direction. After that, the SC-QWR prototype will be installed in a test cryomodule [5] and a cool-down test in the cryomodule will be performed in this fiscal year.

ACKNOWLEDGEMENT

Development of a prototype superconducting resonator and its cryomodule was funded by the ImPACT Program of the Council for Science, Technology and Innovation (Cabinet Office, Government of Japan).

REFERENCES

[1] N. Sakamoto *et al.*, in Proc. SRF2015, WEBA06, (2015) 976.

[2] T. Yanagisawa *et al.*, in Proc. HIAT2015, WEPB17, (2015) 231.

[3] A. Miyamoto *et al.*, in Proc. SRF2015, THPB029, (2015) 1141.

[4] http://www.cst.com

[5] K. Ozeki *et al.*, presented at LINAC2016, East Lansing, USA, September 2016, paper TUPLR061, this conference.